Int j simul model 16 (2017) 4, 658-669
ISSN 1726-4529 Original scientific paper

DYNAMIC CHARACTERISTICS OF COUPLED VEHICLE–TRACK–TUNNEL INTERACTION SYSTEM

Liu, Y.[*]; Liang, B.[**]; Zhao, N. Y.[**] & Wei, S.[***]
[*] School of Civil Engineering, Chongqing Jiaotong University, No. 66 Xuefu Rd., Chongqing, P. R. China
[**] State Key Laboratory of Mountain Bridge and Tunnel Engineering, Chongqing Jiaotong University, No. 66 Xuefu Rd., Chongqing, P. R. China
[***] Faculty of Engineering and Environment, Northumbria University, NE1 8ST, Newcastle, UK
E-Mail: zhny@cqjtu.edu.cn

Abstract
Traditional studies simplify vehicle–track–tunnel system into vehicle–track or vehicle–tunnel models and neglect dynamics influences of vehicle on tunnel through track or track–tunnel on vehicle. This study established the mathematical model of vehicle and finite element model of track–tunnel to disclose vibration characteristics of vehicle–track–tunnel coupled dynamic system. Next, a vehicle–track–tunnel dynamic coupled model was established based on the wheel–rail displacement coordinated relation. Finally, variation laws of vehicle and stress and displacement fields of tunnel surrounding rock when the train travelled at speed of 200 km/h were studied under different track slab stiffness and track structures. Numerical simulation results demonstrate that vehicle vibration indexes change in the linear law with the increase in track slab stiffness. Sleeper embedded ballastless slab track has better damping reduction performance than sleeper buried ballastless slab track. The best damping reduction performance is achieved when the track slab stiffness is 3.5 kPa. The maximum vertical displacement and stress of the tunnel surrounding rock due to vibration at low levels and the tunnel surrounding rock slightly influence vibration indexes of vehicles.
(Received in April 2017, accepted in October 2017. This paper was with the authors 3 months for 1 revision.)

Key Words: Vehicle–Track–Tunnel Coupled System, Equilibrium Equation, Vehicle Motion Quality, Dynamic Characteristics, Track Irregularity

1. INTRODUCTION

High-speed railway is economically efficient, fast, safe, comfortable, and environment-friendly. This railway has outstanding advantages compared with other means of transportation. With the increase in vehicle speed, problems due to vehicle-structure coupled vibration, such as vehicle running quality, infrastructure safety and vibration noises in the surrounding environment, have become increasingly prominent. Vehicle–tunnel coupled vibration problem during vehicle running in a tunnel is extremely important. Thus, studying the coupled dynamic interaction between vehicle and tunnel is the most effective way to explore damping and noise reduction.

Currently, studies on vehicle–tunnel coupled dynamics mainly focus on solving the dynamic equation of vehicle running on an irregular track [1-5], which were summarized into "vehicle dynamics," "track dynamics," and "wheel–track interaction" [5-9]. Established coupling models can be divided into two types, namely vehicle–track system [6] and vehicle–track–roadbed system [7]. These studies did not analyse vehicle and tunnel structure as an integral system and neglected the effects of track–tunnel dynamic properties. The vehicle–track–tunnel coupled vibration problem is complicated due to diversified vehicle structures, track types, track slab stiffness, and tunnel structures. If only mathematical modelling is used and only finite degree of freedom of vehicle structure and wheel–track is considered, then analysing the vibration characteristics of vehicle–track–tunnel coupled system is difficult

when the multimode of track–tunnel structure is neglected. Studies on the dynamic model and characteristics of vehicle–track–tunnel coupled vibration are rare.

Therefore, topics, such as vibration characteristics of vehicle–track–tunnel system and their relationships with vehicle running quality and track–tunnel structure design parameters, have to be focused to increase the riding comfort of vehicles and safety and durability of railway structures and reduce environmental vibrations and noises. In this study, the relationship between vehicle running quality indexes and track–tunnel structural parameters was analysed using the mathematical and finite element modelling analysis of vehicle–track–tunnel system. Moreover, optimization design values of these parameters were discussed. The results provide a theoretical basis to investigate the relationship between tunnel–track structural design parameters and vehicle running quality.

2. LITERATURE REVIEW

Numerous researches on coupled vibration of vehicle–railway and vehicle–roadbed systems have been reported. The main research methodologies include mathematical modelling, numerical simulation, and model testing. Yang et al. and Bhattiprolu et al. established a two-dimensional vehicle–track–roadbed finite element model. They analysed the vehicle running-induced vibration law of roadbed structure using Newmark's step-by-step implicit numerical integration method based on roadbed structural types and vehicle load frequency spectral features. However, they did not analyse the tunnel vibration response [7, 8]. Sadeghi et al. transformed the rail vibration problem into a transfer function, which calculates the frequency/wave velocity of rail and the axial load problems of vehicle, and calculated wheel–rail contact force under the stimulus of track irregularity. They only studied the vehicle–rail coupled solving method [9]. Uzzal et al. and Zhang et al. viewed vibration signals as the combination of periodic vibration through field tests and implemented frequency spectral analysis through Fourier transformation, thereby obtaining the mathematical expression of the vibration acceleration of rail [10, 11]. Lei and Wang introduced the simplified vehicle model, established the kinetic equation of simulated wheel system, and deduced the vibration load of vehicle based on the work of Uzzal et al. However, they did not further analyse the dynamic features of vehicle–track system [12]. Zhai et al. discussed the dynamic features of contact surface between wheel and rail based on wheel–track dynamic interaction and found the best damping reduction and cross-section shape for small-radius curved section of track [13]. Thompson et al. studied noise problem of high-speed trains in tunnels by numerical simulation but did not analyse the relationship between noises and vehicle vibration [14].

Regarding vehicle–tunnel dynamic interaction, Koziol and Hryniewicz obtained vehicle load exciting force curve and power spectrum of track slab and determined time step length and Rayleigh damping coefficient through the vehicle–track coupled model analysis. Moreover, inherent frequency of tunnel structure and surrounding rock system was obtained through modal analysis. However, they did not analyse the vibration law of vehicles [15]. Wei et al. introduced vehicle–track coupled kinetic equation through dynamic stiffness of soft soils, established the vertical random vibration model of subway shield tunnel in soft soil strata and discussed the effects of dynamic stiffness of soft soil on the random vibration of subway shield tunnel. This study only analysed the vibration frequency of tunnel segment structure when the train speed is lower than 120 km/h [16]. Lou and Au, and Amirian et al. established the vehicle–track coupled model based on the Bernoulli–Euler beam principle and the 3D finite element method and calculated longitudinal stress state of a tunnel [17, 18]. Wang et al. simulated vehicle vibration load through the excitation function by using two-dimensional nonlinear finite element method, simulated vehicle vibration load by excitation function, and studied influences of structural form, stiffness, and curvature of tunnel invert on

the stress of tunnel surrounding rock [19]. Liang et al. enlisted tunnel into the vehicle computing model as a substructure and established the vehicle–tunnel coupling dynamic analysis model. They also analysed the dynamic features of tunnel structure and surrounding rock under different surrounding rock levels [20]. The preceding studies mentioned mainly focused on the effects of vehicle vibration on tunnel structure and did not consider vehicle–track–tunnel as an integral system. Studies on vehicle running parameters and vibration characteristics of track-tunnel structure parameters are rare.

The preceding analysis suggests that existing studies mainly focused on vehicle–track–roadbed modelling and its dynamic characteristics, while discussions on the influences of vibration on tunnel structure and surrounding rock are few. Studies on coupling dynamic features of vehicle–track–tunnel system are rare. Based on vehicle dynamic mechanics and numerical simulation, a vehicle–track–tunnel coupling dynamic model was established, and the effects of track type, vehicle structure, wheel mass, steel rail, and wheel on the ratio of wheel–load reduction and vibration features of tunnel surrounding rock were discussed. The remainder of this study is organized as follows. Section 3 describes the vehicle–track–tunnel modelling and its parameters. Section 4 analyses the vertical vibration acceleration of car body, dynamic wheel mass, wheel–load reduction ratio, vertical displacement of rail, and vertical displacement and stress at the top of tunnel surrounding rock. Section 5 draws the conclusions.

3. MODELLING

3.1 Vehicle–track–tunnel mathematical model

In this study, vehicle and track–tunnel systems were viewed as subsystems that interact and mutually couple. Wheel–rail interaction was used as the "link" between the two subsystems. The dynamic features of vehicle–track–tunnel system under varying track structures were analysed by establishing the dynamic equilibrium equation and decoupling of train–track–tunnel system using displacement compatibility condition.

A vehicle with secondary suspension or primary spring suspension was used to study the dynamic response of vehicle–track–tunnel system during high-speed running. Two degrees of freedom (DOF) of drifting and rolling were considered for each car body, and one DOF of drifting was considered for each wheelset. The following hypotheses were derived. (1) The vehicle runs at a constant speed v. (2) Car body and wheelset were considered rigid bodies. (3) The connecting device between two vehicles will not influence vertical and horizontal vibrations of a vehicle. (4) Wheelsets remain in contact with the rail surface throughout the running. The common four-axis vehicle was used as the research object. Figs. 1 and 2 show the mechanical and mathematical models, respectively. The dynamic equilibrium equation of the vehicle is as follows:

$$\begin{bmatrix} M_{ci} & 0 \\ 0 & J_{ci} \end{bmatrix} \begin{Bmatrix} \ddot{Z}_i \\ \ddot{\theta}_i \end{Bmatrix} + \begin{bmatrix} C_{czi} & 0 \\ 0 & C_{c\theta i} \end{bmatrix} \begin{Bmatrix} \dot{Z}_i \\ \dot{\theta}_i \end{Bmatrix} + \begin{bmatrix} K_{czi} & 0 \\ 0 & K_{c\theta i} \end{bmatrix} \begin{Bmatrix} Z_i \\ \theta_i \end{Bmatrix} = \sum_{j=1}^{4} \begin{Bmatrix} K_{wzi} Z_{wij} + C_{wzi} \dot{Z}_{wij} \\ \eta_{ij} l_{ij} \left(K_{wzi} Z_{wij} + C_{wzi} \dot{Z}_{wij} \right) \end{Bmatrix} \quad (1)$$

where M_{ci} and J_{ci} are mass and inertia moment matrices of the vehicle i, respectively; Z_i and θ_i are vertical displacement and corner vector in the centroid of vehicle i, respectively; K_{czi} and C_{czi} are total drifting stiffness and total damping matrices of vehicle i, respectively; $K_{c\theta i}$ and $C_{c\theta i}$ are total rolling stiffness and total damping of vehicle i, respectively; K_{wzi} and C_{wzi} are stiffness and damping of wheelset of vehicle i, respectively; Z_{wij} is the vertical displacement of the wheelset j of vehicle i, l_{ij} is the distance between wheelset j and the centre of vehicle i, and η_{ij} is the sign function of wheelset. η_{ij} is 1 and −1 when j is at the front and rear bogie, respectively.

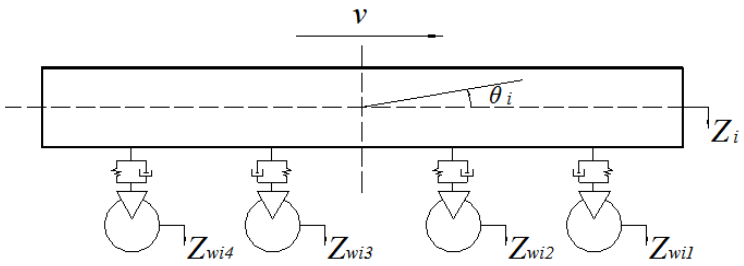

Figure 1: Vehicle model.

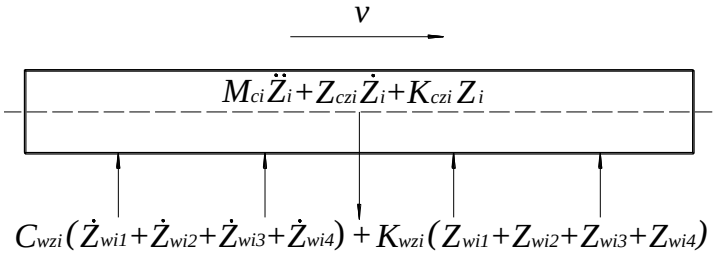

Figure 2: Simplified vehicle model.

Slab track includes sleeper embedded and buried ballastless, they are commonly used in high-speed railway. Slab track and tunnel were considered as an integral substructure. The track–tunnel 3D finite element model was established.

In the sleeper embedded ballastless track, rubber boots are installed at the double-block type or lower part and the surrounding places of two independent rest pads. Subsequently, an elastic cushion is paved between the bottom of the pad and boots. Then, it is shaped by pouring concrete mortar on its surrounding and below double sleepers. This track has a damping reduction performance. The track structure is shown in Fig. 3.

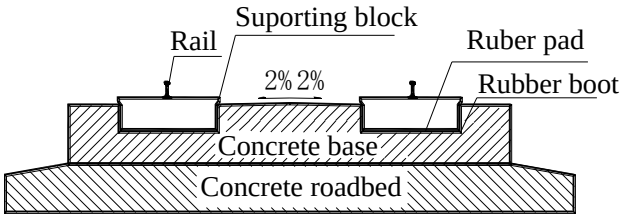

Figure 3: Cross section of sleeper embedded ballastless track.

In sleeper buried ballastless track, concrete mortar in site is poured into a pre-fabricated integral or double-block sleeper. Then, sleepers are buried into a concrete roadbed or "vibrated" into the concrete roadbed plate; thus, the sleeper and the concrete roadbed plate form an integral form. Fig. 4 shows the track structure.

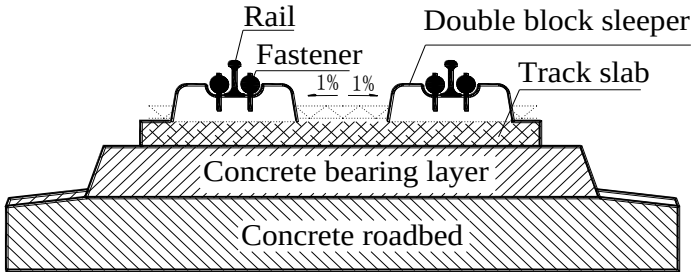

Figure 4: Cross section of sleeper buried ballastless track.

The track–tunnel model was established according to the substructure method. During computation, free vibration frequencies and vibration mode of this substructure could be

obtained first. Then, coupling vehicle and track–tunnel vibration equations were converted into independent modal equations. The low-orders of vibration modes were selected in the computation because the vibration of structures is mainly controlled by several low-order vibration modes [4, 5]. Therefore, only orders of vibration mode at contact point between wheelset and rail or rail nodes were analysed. In the computation, vibration variables, namely $C_n = 2\xi_n\omega_n / M_n$ and $K_n = \omega_n^2 / M_n$, were introduced. Finally, the track–tunnel vibration equation was obtained:

$$\ddot{A}_n + 2\xi_n\omega_n\dot{A}_n + \omega_n^2 A_n = F_n \tag{2}$$

where F_n is the generalized force that acts on the *n*-order vibration mode of the track–tunnel system; A_n is the corresponding generalized coordinates (generalized displacement at one time-step); M_n, C_n, and K_n are generalized mass, damping, and stiffness, respectively; ω_n is the angular frequency of *n*-order vibration mode; and ξ_n is the damping ratio of *n*-order vibration mode.

According to the hypothesis, the vertical displacement of wheelset and rail surface during vehicle running are mutually coupling. The vertical displacement of wheelset (Z_{wij}) is the sum of track irregularity value $Z_s(x_{ij})$ and vertical displacement of track–tunnel vibration $Z_r(x_{ij})$. The vertical displacement at any track–tunnel section $Z_r(x_{ij})$ can be obtained by the superposition of several vibration functions. The displacement coordination equation of the vehicle–track–tunnel system can be established based on the computation of the first *n*-orders of vibration mode:

$$Z_{wij} = \sum_{n=1}^{N} A_n \Phi_n\left(x_{ij}\right) + Z_s\left(x_{ij}\right) \tag{3}$$

where $\Phi_n(x)$ is the *n*-order of vibration function at one position, $Z_s(x_{ij})$ is the vertical irregularity at x_i of the rail surface and is a simulated value, x_{ij} is the horizontal coordinate of the wheelset *j* of vehicle *i* on the rail surface.

According to the displacement compatibility condition of vehicle–track–tunnel vibration, Eqs. (1) and (2) are combined and Eq. (3) is integrated into their simultaneous equation to obtain the vertical vibration equation set of the vehicle–tunnel system as follows:

$$\begin{cases} \begin{bmatrix} M_{ci} & 0 \\ 0 & J_{ci} \end{bmatrix} \begin{Bmatrix} \ddot{Z}_i \\ \ddot{\theta}_i \end{Bmatrix} + \begin{bmatrix} C_{czi} & 0 \\ 0 & C_{c\theta i} \end{bmatrix} \begin{Bmatrix} \dot{Z}_i \\ \dot{\theta}_i \end{Bmatrix} + \begin{bmatrix} K_{czi} & 0 \\ 0 & K_{c\theta i} \end{bmatrix} \begin{Bmatrix} Z_i \\ \theta_i \end{Bmatrix} = \sum_{j=1}^{4} \begin{Bmatrix} K_{wzi}\left[\sum_{n=1}^{N} A_n\Phi_n\left(x_{ij}\right) + Z_s\left(x_{ij}\right)\right] + C_{wzi}\left[\sum_{n=1}^{N} \dot{A}_n\Phi_n\left(x_{ij}\right) + \dot{Z}_s\left(x_{ij}\right)\right] \\ \eta_{ij}l_{ij}\left[K_{wzi}\left(\sum_{n=1}^{N} A_n\Phi_n\left(x_{ij}\right) + Z_s\left(x_{ij}\right)\right) + C_{wzi}\left(\sum_{n=1}^{N} \dot{A}_n\Phi_n\left(x_{ij}\right) + \dot{Z}_s\left(x_{ij}\right)\right)\right] \end{Bmatrix} \\ \ddot{A}_n + 2\xi_n\omega_n\dot{A}_n + \omega_n^2 A_n = \sum_{i=1}^{N_c}\sum_{j=1}^{4} \Phi_n\left(x_{ij}\right) \begin{Bmatrix} \left(\frac{1}{4}M_{ci} + M_{wi}\right)g + K_{wzi}\left(Z_i + \eta_{ij}l_{ij}\theta_i\right) + C_{wzi}\left(\dot{Z}_i + \eta_{ij}l_{ij}\dot{\theta}_i\right) \\ -M_{wi}\left[\sum_{n=1}^{N} \ddot{A}_n\Phi_n\left(x_{ij}\right) + \ddot{Z}_s\left(x_{ij}\right)\right] \end{Bmatrix} \end{cases} \tag{4}$$

where M_{wi} is the wheelset mass of vehicle *i*, and other signs are the same as in the previous equation.

Eq. (4) is the coupled dynamic equation set of vehicle–track–tunnel system. This equation contains a total of $2N_c + N$ equations, where N_c is the number of vehicles on the track, and N is number of modal equation sets of track–tunnel submodels. Superposing several representative groups of low-order vibration modes is necessary. The vibration equation set is solved through the Newmark–β method.

3.2 Track–tunnel finite element model

Although tunnel is in a semi-infinite space, the influence zone of vehicle–tunnel system vibration can be separated and discredited, and the vehicle–tunnel system model in the finite space was established. The cut surface of the model's boundaries, that is, artificial boundary,

does not exist in the original continuous medium. Therefore, the geometric size of the 3D finite element model can be thrice the hole height over the tunnel arc along the horizontal direction, and the tunnel bottom was larger than the hole height. According to existing experimental data and computing parameters, the longitudinal length of the model should be at least 24 sleeper bays to ensure computing accuracy [3-6]. In the established model, the longitudinal length of the tunnel was 50 m. The constraints of the artificial boundary in the model include horizontal constraint at the side surface and fixed constraint at the bottom surface. The upper surface was a free boundary. For the convenience of calculation analysis, 10 m buried depth of tunnel, III-level surrounding rock conditions, and composite lining (primary lining thickness = 30 cm and secondary lining thickness = 50 cm) were determined.

Fig. 5 shows the cross sections of tunnel and track structures. Table I presents the computing parameters of the materials.

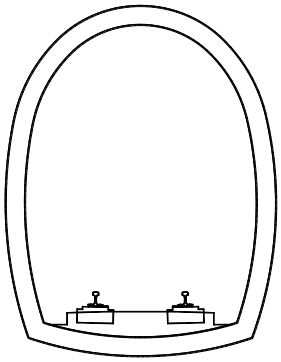

Figure 5: Cross section of the tunnel.

Table I: Computing parameters of materials.

Materials	**Elasticity modulus** (GPa)	**Density** (kg/m^3)	**Poisson's ratio**	**Cohesion** (MPa)	**Internal friction angle** (°)
Surrounding rock	2.9	2200	0.30	0.25	40
Primary lining	29.50	2500	0.22	—	—
Secondary lining	31	2500	0.20	—	—

Slab track comprises steel rail, fastener, rubber pad, concrete slabs, isolated layer, and concrete bed. The coordinated working properties and influences of parameter changes of the model unit were selected to consider dynamic relations of the railway–tunnel model. (1) Tunnel lining and surrounding rock were simulated by solid45 unit in the entity unit. For boundary conditions, X- and Z-directional constraints were applied at two sides, Y- and Z-directional constraints were applied at the bottom, and Z-directional constraint was applied in the front and back surfaces. (2) Steel rails were viewed as beams based on the elastic foundation and simulated by Beam 189 unit in the beam unit. (3) In the integral roadbed of ballastless track, sleepers and the integral roadbed were simulated by solid45 unit in beam entity unit. (4) Fasteners were simulated by the spring damping unit COMBIN14. These fasteners have consistent vertical tension and compressive stiffness. Static rigidity was 10–40 kN/mm. All the stiffness values in the model were multiplied by the dynamic-static ratio (1.5).

3.3 Vehicle parameters

The mechanism of structural damping is complicated. The dynamic response of structures with damping was smaller than that of the structure without damping. Therefore, damping size significantly influences the dynamic characteristics of the structure. According to existing experimental data and research results of high-speed railway [15], the computing parameters of the selected vehicle model are shown in Table II.

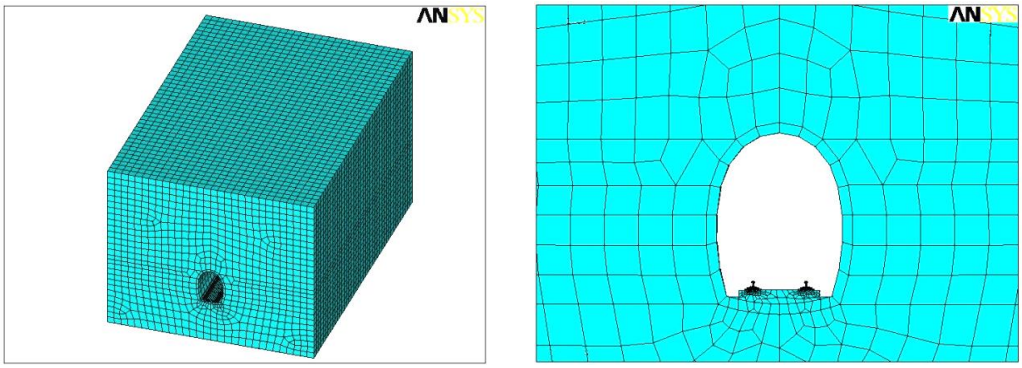

Figure 6: Track–tunnel finite element model.

Table II: Parameters of vehicle model.

Parameters	Sign	Unit	Value
Car body mass	M_{ci}	kg	54200
Rolling inertia of car body	J_{cj}	kg·m^2	3316352
Wheelset mass	M_{wi}	kg	1900
Inertia of wheelset	—	kg·m^2	138
Spring stiffness of wheelset	K_{wzij}	kN/m	1140
Damping coefficient of wheelset	C_{wzij}	kN·s/m	10
Number of wheelsets	N_i	set	4
Total stiffness of vehicle drifting	K_{czi}	kN/m	1140 × 4
Total damping coefficient of vehicle drifting	$K_{c\varphi i}$	kN·m	320564.352
Total damping coefficient of vehicle rolling	C_{czi}	kN·s/m	10 × 4
Length of vehicle	$C_{c\varphi i}$	kN·s·m	2812
Distance between inner wheel to centre of the vehicle	L_{ci}	m	26.58
Wheelbase of wheelset	L_{ij}	m	7.72

In Table II, the rolling stiffness of the vehicle is:

$$K_{c\phi i} = 2K_{wzi}L_{ij}^2 + 2K_{wzi}(L_{ij} + L_w)^2 + 2K_{wzi}(L_{ij} + 2L_w)^2 \tag{5}$$

while the rolling damping of the vehicle is:

$$C_{c\phi i} = 2C_{wzi}L_{ij}^2 + 2C_{wzi}(L_{ij} + L_w)^2 + 2C_{wzi}(L_{ij} + 2L_w)^2 \tag{6}$$

First, the modal analysis was carried out based on the 3D finite element tunnel–track model. The modal state was extracted using the Block Lanczos method to obtain the natural frequency of vibration and vector. Next, the vehicle–track–tunnel dynamic equilibrium equation was decoupled through displacement compatibility conditions, and vehicle–track–tunnel coupled vibration response due to excitation (geometric irregularity) of the wheel–rail system was analysed.

4. SIMULATION RESULT AND DISCUSSION

4.1 Main indexes of vehicle–track–tunnel system

The dynamic interaction mechanism of the vehicle–track–tunnel system is complicated. In this study, the design parameters that can reflect the running quality of the vehicle and the track–tunnel structure or indexes of the dynamic features were investigated, including the vertical vibration acceleration of vehicle $\ddot{Z}_c$ (m/s^2), dynamic wheel weight of vehicle P_{ijw}

(kN), ratio of wheel–load reduction D_j, vertical displacement of rail Z_r (mm), vertical displacement at the top of tunnel surrounding rock Z_f (mm), and vertical stress at the top of tunnel surrounding rock σ_f (MPa).

The vertical vibration acceleration of different vehicles can be calculated from the decoupling of Eq. (1).

When the rail contact with wheelset *j* of vehicle *i* is analysed, this wheelset bears its own weight, vertical forces from spring and damping, and its own inertia force and counterforce from rail contact points. These forces help the wheelset achieve a dynamic balance state. Fig. 7 illustrates the mechanical model.

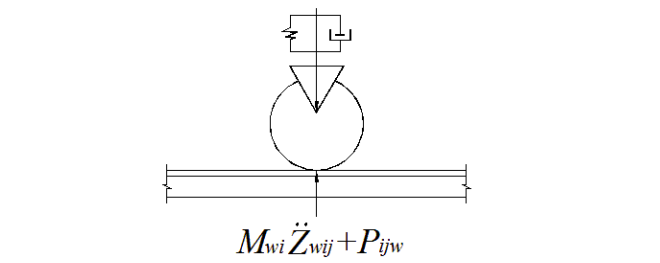

Figure 7: Analysis of motion forces on wheelset.

Based on the drifting equilibrium equation of wheelsets, the acting force of each wheelset on rails is:

$$P_{ijw}=P_{ijs}+K_{wzi}\left(Z_{wij}+\eta_{ij}l_{ij}\theta_i\right)+C_{wzi}\left(\dot{Z}_{wij}+\eta_{ij}l_{ij}\dot{\theta}_i\right)-M_{wi}\ddot{Z}_{wij} \tag{7}$$

where P_{ijs} is the static wheel weight of vehicle, M_{wi} is the wheelset mass of vehicle *i*, $P_{ijs}=g\,(1/6\,M_{ci}+M_{wi})$ for haulage motor, and $P_{ijs}=g\,(1/4\,M_{ci}+M_{wi})$ for trail vehicle. Z_{wij} is the vertical displacement of wheelset *j* of vehicle *i*, and P_{ijw} is the counterforce of rails to the wheelset *j* of vehicle *i*.

The axial ratio of wheel–load reduction of the wheelset *j* of vehicle *i* is:

$$D_j=\frac{p_{ijw}-p_{ijs}}{p_{ijs}}=\frac{p_{ijw}}{p_{ijs}}-1 \tag{8}$$

where p_{ijw} is the dynamic wheel weight, and p_{ijs} is the average static wheel weight.

The vertical displacement $Z_r(x)$ at any cross section of track–roadbed system can be obtained by the superposition of several modal functions. If the first *n*-order vibration modes were selected in computation, then:

$$Z_r\left(x\right)=\sum_{n=1}^{N}A_n\Phi_n\left(x\right) \tag{9}$$

where $\Phi_n(x)$ is the *n*-order vibration function at one position, A_n is the corresponding generalized coordinates (generalized displacement under a few time-steps), and *x* is the horizontal position at one section.

Vertical displacement Z_f and vertical stress σ_f can be calculated from the exciting force of wheelset (dynamic wheel weight of vehicle in Eq. (4)) through the dynamic finite element method.

4.2 Dynamic characteristics of vehicle–track–tunnel system

A U-shaped tunnel under III-level surrounding rock conditions was selected. When the train speed was 200 km/h, the wheel loads for sleeper embedded and sleeper buried ballastless tracks were calculated through the vehicle–track–tunnel model with variation of track slab

(Elasticity modulus = 2, 2.5, 3.5, 4 and 5 kPa). Subsequently, dynamic numerical calculation of the tunnel was conducted. The effects of track on $\ddot{Z}_c$, P_{ijw}, D_j, Z_r, Z_f, and σ_f were analysed.

Fig. 8 shows that 1) the maximum $\ddot{Z}_c$ increases with the increase in track slab stiffness. $\ddot{Z}_c$ is maintained at a reasonable level, which is lower than the discrimination standard of Japan's East Sea Route (2.5 m/s^2). 2) The maximum $\ddot{Z}_c$ significantly increases in the range of track slab stiffness (2.0 – 3.5 kPa) but becomes stable in the range of 3.5 – 6.0 kPa. 3) The vehicle vibration acceleration under sleeper embedded ballastless track is smaller than that under sleeper buried ballastless track because the former has rubber boots and an elastic cushion layer, which can reduce vibration.

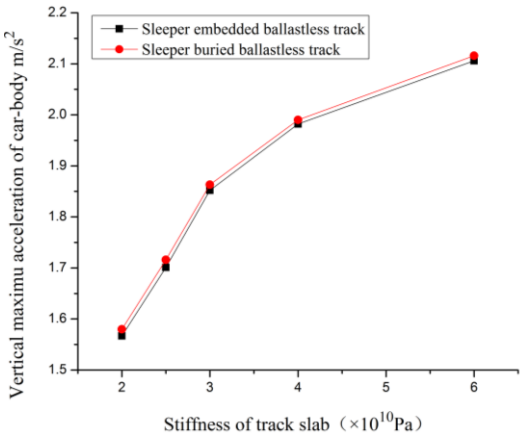

Figure 8: Effects of track type and track slab stiffness on the maximum vertical acceleration of car body.

Figs. 9 and 10 demonstrate that 1) the maximum P_{ijw} and D_j increase with the increase in track slab stiffness. The values of these variables are lower than discrimination standards of irregularity safety and comfort of high-speed railways (250 kN and 0.6, respectively) [13]. 2) The sleeper embedded ballastless track has good damping reduction performance because it comprises rubber boots and an elastic cushion layer. Therefore, maximum P_{ijw} and D_j under sleeper embedded ballastless track are smaller than those under sleeper buried ballastless track.

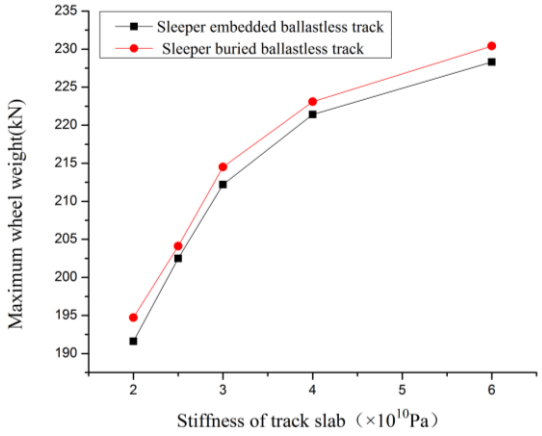

Figure 9: Effects of track type and track slab stiffness on maximum P_{ijw}.

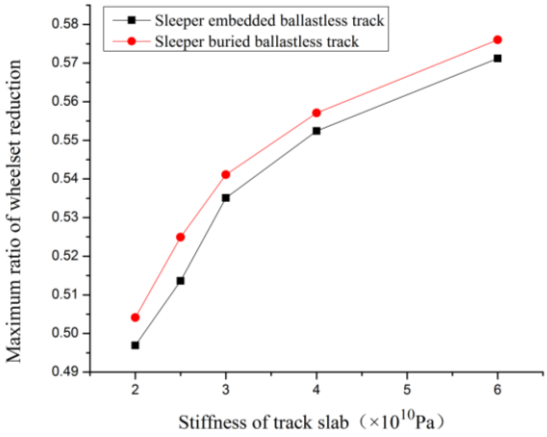

Figure 10: Effects of track type and track slab stiffness on maximum D_j.

Fig. 11 shows that 1) the maximum Z_r decreases with the increase in track slab stiffness, and its value is lower than 0.5 mm. This finding completely conforms to the design standard

($Z_r \leq 2$ mm) [13]. 2) Sleeper embedded ballastless track has good damping reduction performance.

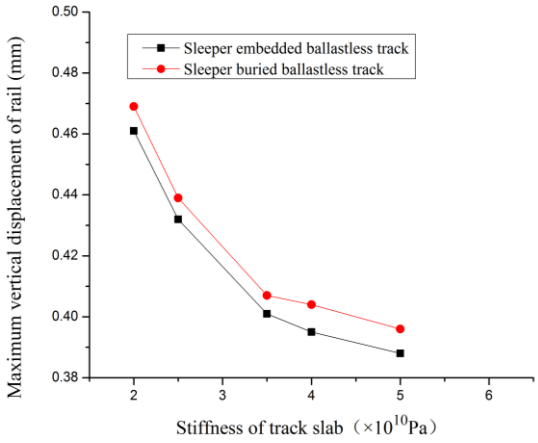

Figure 11: Effects of railway type and stiffness of track slab on Z_r.

Figs. 12 and 13 show that 1) the maximum Z_f and σ_f decrease with the increase in track slab stiffness, that is, their values are lower than 0.15 mm and 1.5 MPa, respectively. 2) Owing to the superior damping reduction performance of the sleeper embedded ballastless track, its maximum Z_f and σ_f are smaller than those under sleeper buried ballastless track with similar conditions.

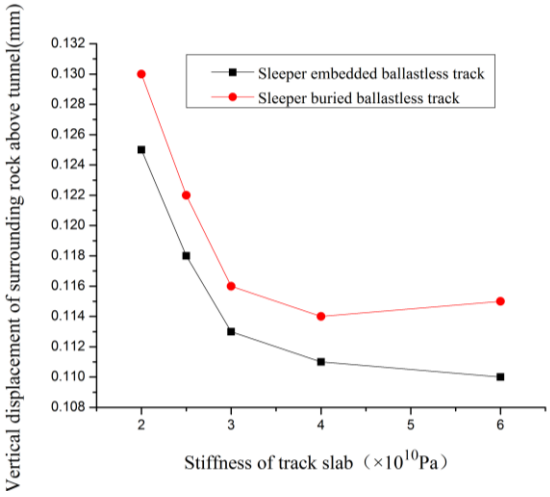

Figure 12: Effects of track type and track slab stiffness on maximum Z_f.

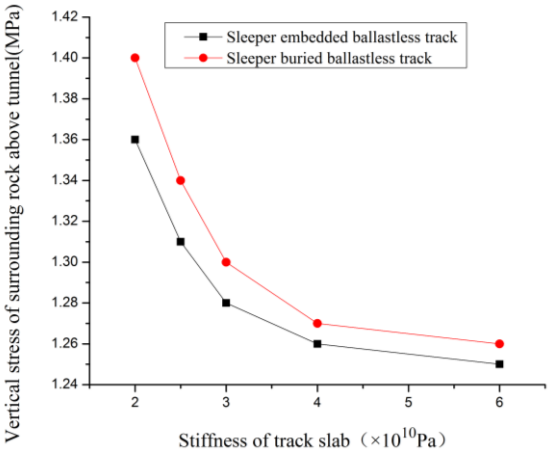

Figure 13: Effects of track type and stiffness of track slab on maximum σ_f.

5. CONCLUSIONS

This study established the vehicle–track–tunnel model by combining the mathematical vehicle and finite element submodels of track–tunnel system to disclose the vibration characteristics of vehicle–track–tunnel system under coupled dynamic interaction. Moreover, the coupled dynamic equation of the vehicle–track–tunnel model was solved based on wheel–rail interaction relationship. Factors, such as vertical vibration acceleration of the vehicle, dynamic wheel weight, ratio of wheel–load reduction, vertical displacement of rail, vertical displacement and stress at the top of the tunnel surrounding rock which affects the running quality of vehicles, and dynamic characteristics of the railway–tunnel structure, were analysed. The following conclusions could be drawn.

(1) Owing to the same type of track slab, namely sleeper embedded and buried ballastless tracks, all indexes generally present linear increase or reduction with the increase in track slab stiffness. The stiffness of the track slab has a slight influence on the safety indexes of driving vehicles and tunnel/track.

(2) Owing to the same track slab stiffness, the indexes of sleeper embedded ballastless track are superior to those of sleeper buried ballastless track, thereby indicating that the sleeper embedded ballastless track has better damping reduction performance.

(3) With comprehensive considerations to design standards of indexes, adopting sleeper embedded ballastless track is suggested. The appropriate stiffness of track slab is 3.5 kPa. This value can meet various running indexes and would not blindly increase track slab stiffness to increase stress performance of tunnel, thus causing wastes.

(4) When vehicles travel in tunnels with III-level surrounding rock, the maximum vertical displacement and stress at the top of the tunnel surrounding rock are still maintained at a low level.

Mathematical and finite element models are combined in this study. Vehicle, track–tunnel, and vehicle–track–tunnel coupled system models are constructed. The parameters in these models are based on engineering practices to accurately reflect the actual vehicle running in tunnels. Research conclusions have important guiding significance to establish the matching relationship between track–tunnel structural design parameters and running quality of vehicle and evaluate the vibration influence of surrounding environment. The conclusions in this study still have limitations in investigating the acceleration and braking of vehicle in tunnel because the established models are based on the uniform motion of vehicle. Further studies can be carried out by adding acceleration parameters in the vehicle model.

ACKNOWLEDGEMENT

This work was in part financially supported by two grants from Projects in Management funded by the National Nature Science Foundation of China (51608081), and Foundation of State Key Laboratory of Mountain Bridge and Tunnel Engineering of China (CQSLBF-Y16-18).

REFERENCES

[1] Nielsen, J. C. O.; Igeland, A. (1995). Vertical dynamic interaction between train and track-influence of wheel and track imperfections, *Journal of Sound and Vibration*, Vol. 187, No. 5, 825-839, doi:10.1006/jsvi.1995.0566

[2] Liang, B.; Luo, H.; Ma, X. (2007). Dynamic model of the vehicle-subgrade coupled system under secondary suspension, *Applied Mathematics and Mechanics*, Vol. 28, No. 6, 769-778, doi:10.1007/s10483-007-0607-z

[3] Liang, B.; Zhu, D.; Cai, Y. (2001). Dynamic analysis of the vehicle-subgrade model of vertical coupled system, *Journal of Sound and Vibration*, Vol. 245, No. 1, 79-92, doi:10.1006/jsvi.2000.3547

[4] Esmailzadeh, E.; Jalili, N. (2003). Vehicle-passenger-structure interaction of uniform bridges traversed by moving vehicles, *Journal of Sound and Vibration*, Vol. 260, No. 4, 611-635, doi:10.1016/S0022-460X(02)00960-4

[5] Zhang, Z. C.; Lin, J. H.; Zhang, Y. H.; Howson, W. P.; Williams, F. W. (2010). Non-stationary random vibration analysis of three-dimensional train–bridge systems, *Vehicle System Dynamics*, Vol. 48, No. 4, 457-480, doi:10.1080/00423110902866926

[6] Sadeghi, J.; Fesharaki, M. (2013). Importance of nonlinearity of track support system in modeling of railway track dynamics, *International Journal of Structural Stability and Dynamics*, Vol. 13, No. 1, Paper 1350008, 16 pages, doi:10.1142/S0219455413500089

[7] Yang, S.-P.; Li, S.-H.; Lu, Y.-J. (2010). Investigation on dynamical interaction between a heavy vehicle and road pavement, *Vehicle System Dynamics*, Vol. 48, No. 8, 923-944, doi:10.1080/00423110903243166

[8] Bhattiprolu, U.; Bajaj, A. K.; Davies, P. (2013). An efficient solution methodology to study the response of a beam on viscoelastic and nonlinear unilateral foundation: Static response, *International Journal of Solids and Structures*, Vol. 50, No. 14-15, 2328-2339, doi:10.1016/j.ijsolstr.2013.03.014

[9] Sadeghi, J.; Khajehdezfuly, A.; Esmaeili, M.; Poorveis, D. (2016). Dynamic interaction of vehicle and discontinuous slab track considering nonlinear Hertz contact model, *Journal of Transportation Engineering*, Vol. 142, No. 4, 11 pages, doi:10.1061/(ASCE)TE.1943-5436.0000823

[10] Uzzal, R. U. A.; Ahmed, A. K. W.; Bhat, R. B. (2013). Modelling, validation and analysis of a three-dimensional railway vehicle–track system model with linear and nonlinear track properties in the presence of wheel flats, *Vehicle System Dynamics*, Vol. 51, No. 11, 1695-1721, doi:10.1080/00423114.2013.822987

[11] Zhang, Z.; Wei, S.; Andrawes, B.; Kuchma, D. A.; Edwards, J. R. (2016). Numerical and experimental study on dynamic behaviour of concrete sleeper track caused by wheel flat, *International Journal of Rail Transportation*, Vol. 4, No. 1, 1-19, doi:10.1080/23248378.2015.1123657

[12] Lei, X.; Wang, J. (2014). Dynamic analysis of the train and slab track coupling system with finite elements in a moving frame of reference, *Journal of Vibration and Control*, Vol. 20, No. 9, 1301-1317, doi:10.1177/1077546313480540

[13] Zhai, W.; Gao, J.; Liu, P.; Wang, K. (2014). Reducing rail side wear on heavy-haul railway curves based on wheel-rail dynamic interaction, *Vehicle System Dynamics*, Vol. 52, Suppl. 1, 440-454, doi:10.1080/00423114.2014.906633

[14] Thompson, D. J.; Latorre Iglesias, E.; Liu, X.; Zhu, J.; Hu, Z. (2015). Recent developments in the prediction and control of aerodynamic noise from high-speed trains, *International Journal of Rail Transportation*, Vol. 3, No. 3, 119-150, doi:10.1080/23248378.2015.1052996

[15] Koziol, P.; Hryniewicz, Z. (2012). Dynamic response of a beam resting on a nonlinear foundation to a moving load: Coiflet-based solution, *Shock and Vibration*, Vol. 19, No. 5, 995-1007, doi:10.3233/SAV-2012-0706

[16] Wei, K.; Zhai, W.; Xiao, J. (2014). Vertical random vibration model for subway shield tunnel in soft soil, *Engineering Mechanics*, Vol. 31, No. 6, 117-123

[17] Lou, P.; Au, F. T. K. (2013). Finite element formulae for internal forces of Bernoulli-Euler beams under moving vehicles, *Journal of Sound and Vibration*, Vol. 332, No. 6, 1533-1552, doi:10.1016/j.jsv.2012.11.011

[18] Amirian, B.; Hosseini-Ara, R.; Moosavi, H. (2014). Surface and thermal effects on vibration of embedded alumina nanobeams based on novel Timoshenko beam model, *Applied Mathematics and Mechanics*, Vol. 35, No. 7, 875-886, doi:10.1007/s10483-014-1835-9

[19] Wang, X.; Yang, L.; Zhou, Z. (2006). Dynamic response analysis of lining structure for tunnel under vibration loads of train, *Chinese Journal of Rock Mechanics and Engineering*, Vol. 25, No. 7, 1337-1342

[20] Liang, B.; Liu, Y.; Qing, W.; Luo, H. (2014). Influence of surrounding rock grades on the system dynamic properties under the vehicle-tunnel coupling, *Chinese Journal of Underground Space and Engineering*, Vol. 10, No. 1, 77-83